FLORE
Repository istituzionale dell'Università degli Studi di Firenze

Increased susceptibility to amyloid toxicity in familial Alzheimer's fibroblasts

Questa è la Versione finale referata (Post print/Accepted manuscript) della seguente pubblicazione:

Original Citation:

Increased susceptibility to amyloid toxicity in familial Alzheimer's fibroblasts / C. Cecchi; C. Fiorillo; S. Baglioni; A. Pensalfini; S. Bagnoli; B. Nacmias; S. Sorbi; D. Nosi ; A. Relini; G. Liguri. - In: NEUROBIOLOGY OF AGING. - ISSN 0197-4580. - STAMPA. - 28:(2007), pp. 863-876.

Availability:

This version is available at: 2158/23991 since:

Terms of use:

Open Access

La pubblicazione è resa disponibile sotto le norme e i termini della licenza di deposito, secondo quanto stabilito dalla Policy per l'accesso aperto dell'Università degli Studi di Firenze (https://www.sba.unifi.it/upload/policy-oa-2016-1.pdf)

Publisher copyright claim:

(Article begins on next page)

05 May 2023

ELSEVIER

Neurobiology of Aging 28 (2007) 863–876

NEUROBIOLOGY OF AGING

www.elsevier.com/locate/neuaging

Increased susceptibility to amyloid toxicity in familial Alzheimer's fibroblasts

Cristina Cecchi [a,*], Claudia Fiorillo [a], Serena Baglioni [a], Anna Pensalfini [a], Silvia Bagnoli [b], Benedetta Nacmias [b], Sandro Sorbi [b], Daniele Nosi [c], Annalisa Relini [d], Gianfranco Liguri [a]

[a] *Department of Biochemical Sciences, University of Florence, viale Morgagni 50, 50134 Florence, Italy*
[b] *Department of Neurological and Psychiatric Sciences, University of Florence, viale Pieraccini 6, 50139 Florence, Italy*
[c] *Department of Anatomy, Histology and Forensic Medicine, University of Florence, viale Morgagni 85, 50134 Florence, Italy*
[d] *Department of Physics, University of Genoa, via Dodecaneso 33, I-16146 Genoa, Italy*

Received 8 June 2005; received in revised form 14 April 2006; accepted 3 May 2006
Available online 15 June 2006

Abstract

Much experimental evidence suggests that an imbalance in cellular redox status is a major factor in the pathogenesis of Alzheimer's disease (AD). Our previous data showed a marked increase in membrane lipoperoxidation in primary fibroblasts from familial AD (FAD) patients. In the present study, we demonstrate that when oligomeric structures of Aβ 1-40 and Aβ 1-42 are added to the culture media, they accumulate quicker near the plasma membrane, and are internalized faster and mostly in APPV717I fibroblasts than in age-matched healthy cells; this results in an earlier and sharper increase in the production of reactive oxygen species (ROS). Higher ROS production leads in turn to an increase in membrane oxidative-injury and significant impairment of cellular antioxidant capacity, giving rise to apoptotic cascade activation and finally to a necrotic outcome. In contrast, healthy fibroblasts appear more resistant to amyloid oxidative-attack, possibly as a result of their plasma membrane integrity and powerful antioxidant capacity. Our data are consistent with increasing evidence that prefibrillar aggregates, compared to mature fibrils, are likely the more toxic species of the peptides. These findings provide compelling evidence that cells bearing increased membrane lipoperoxidation are more susceptible to aggregate toxicity as a result of their reduced ability to counteract amyloid oligomeric attack.
© 2006 Elsevier Inc. All rights reserved.

Keywords: Familial Alzheimer's disease; APP and PS-1 genes; Amyloid β-peptide; Fibroblasts; Oxidative stress; Antioxidant capacity; Lipid peroxidation; Amyloid aggregate toxicity

1. Introduction

A neuropathological characteristic of Alzheimer's disease (AD) is the extracellular accumulation of amyloid beta peptide (Aβ) in neuritic plaques, whose appearance can precede by decades the onset of symptoms [49]. Aβ deposits in AD patients are almost exclusively composed of the highly amyloidogenic 1-42 form (Aβ 1-42), which is normally produced by cells in much lower quantities than the 40 residues form (Aβ 1-40). Aβ 1-42 is more prone to aggregation *in vitro* than Aβ 1-40, and its cytotoxicity is considered to be the main cause of neuronal impairment in AD. In familial Alzheimer's disease (FAD) patients, an early increase has been reported in the production of Aβ 1-42 arising from intracellular processing of amyloid precursor protein (APP) [63]. Interestingly, all the observed mutations associated with FAD cases lead independently to an increased production of Aβ [18,58]. Autosomal dominant forms of FAD are often determined by

Abbreviations: Aβ, amyloid β-peptide; ABTS, 2,2′-azino-di-3-ethylbenzthiazoline sulphonate; AD, Alzheimer's disease; APP, amyloid precursor protein; CM-H_2,DCFDA, 2′,7′-dichlorodihydrofluorescein diacetate; ECL, enhanced chemiluminescence; FAD, familial Alzheimer's disease; GSH, glutathione; 4-HNE, 4-hydroxy-2-nonenal; MDA, malondialdehyde; PBS, phosphate buffer saline; PMSF, phenylmethylsulphonylfluoride; PS, presenilin; ROS, reactive oxygen species; TAC, total antioxidant capacity; ThT, thioflavine; TM-AFM, tapping mode atomic force microscopy

* Corresponding author. Tel.: +39 055 4598320; fax: +39 055 4598905.
E-mail address: cristina.cecchi@unifi.it (C. Cecchi).

0197-4580/$ – see front matter © 2006 Elsevier Inc. All rights reserved.
doi:10.1016/j.neurobiolaging.2006.05.014

specific mutations in the APP gene located on chromosome 21, or in the genes mapped on chromosomes 14 and 1, encoding presenilin-1 (PS-1) and presenilin-2 (PS-2) respectively, which are components of a large protein complex responsible for γ-secretase activity [20]. Although FAD is a minority (less than 5%) of AD cases, these data point to a pathogenetic role for the metabolism of APP and for the deposition of Aβ. This in turn suggests a role for Aβ in the non-genetic AD forms, since the pathological endpoint and hallmarks of familial and sporadic AD are very similar.

Recent remarkable findings from research teams worldwide, of protein aggregation as a common key feature in several neurodegenerative diseases, constitute progress in understanding the basic mechanism of the so-called "amyloid hypothesis" of AD [29]. The amyloid hypothesis is supported by *in vivo* and *in vitro* evidence concerning several amyloidogenic proteins that indicates a direct cytotoxic effect of amyloid aggregates. Abundant data show that the prefibrillar species of Aβ peptides and of other amyloidogenic proteins such as alpha-synuclein or transthyretin, which are formed early in the process of fibrillogenesis, are neurotoxic, whereas the mature fibrils are much less toxic [11,35,38,42,61,69]. It has recently been found that prefibrillar aggregates, but not mature fibrils from proteins not involved in amyloid diseases can impair cell viability when added to cultured cell media [7,14]. It follows that the cross-β fold is not only the structural feature common to all amyloid aggregates, but is also the structural determinant of cytotoxicity of any amyloid aggregate. There is evidence that protein conversion into toxic aggregates is enhanced by cellular membranes and that self-assembly on the bilayer surface is critical for membrane disruption [4]. A leading theory concerning the molecular basis of amyloid toxicity is that a sub-population of prefibrillar aggregates, assembled in pore-like fashion, interacts with cell membranes and provides them with non-specific pores leading to free Ca^{2+} homeostasis imbalance [61,26,40]. The rise in free calcium is usually coupled to a marked increase in reactive oxygen species (ROS). This is a result of the activation of oxidative metabolism following the increased need for ATP required by the calcium pumps to clear the excess free Ca^{2+} [53]. ROS increase may in turn reinforce the increase in free Ca^{2+}, of which extrusion from the cytosol is inhibited by calcium pump oxidation. Other studies have shown that the role of methionine 35 (Met-35), in conjunction with the secondary structure of the Aβ 1-42 itself, is critical for the oxidative and neurotoxic properties of the peptide [10]. Mutagenesis studies on the C-terminal helical region of the peptide suggest that presence of Aβ 1-42 in the lipid bilayer is necessary for induction of Met-35 lipid peroxidation and subsequent neurotoxicity. Several lines of evidence support the possibility that interactions of Aβ peptide causes mitochondrial damage upon translocation of protofibrils to the membranes [31]. Mitochondria are the major subcellular source of superoxide anion radical, which can interact with nitric oxide (NO) to form peroxynitrite [12,71]. ROS and peroxynitrite accumulation results in damage to major macromolecules in cells, including lipids, proteins and nucleic acids [47,60,62,68]. The lipoperoxidation process could influence the pathogenesis of AD [55,59]. Indeed, 4-hydroxynonenal (4-HNE), which is one of the most reactive end products of lipoperoxidation, appears to induce neuronal death upon binding to proteins by altering important transporter proteins, such as the ATPases involved in calcium homeostasis and the glutamate transporter EAAT2 [10,52]. The healthy brain is protected from oxidative injury by antioxidant defences that include antioxidant enzymes and free radical scavengers. Many recent investigations have strengthened the hypothesis that an impairment in cellular total antioxidant capacity (TAC) plays a central role in AD [47,46]. Recently, we have found that lymphoblasts and fibroblasts carrying APP and PS-1 gene mutations have a significant TAC impairment compared to healthy controls [15].

The data reported in the last few years have considerably improved our knowledge of the molecular basis of protein aggregation into amyloid assemblies, and of the relation between aggregate structure and toxicity to exposed cells [23]. However, one of the intriguing issues that have not been elucidated is the pathological role of each specific Aβ aggregates in AD brain areas. Studies on autopsied brain tissue cannot reveal the early biochemical anomalies induced by various forms of Aβ aggregates, so we carried out a study of cultured skin fibroblasts from FAD patients bearing either APP or PS-1 gene mutations, and age-matched healthy control cells whose culture medium was supplemented by a fixed amount of amyloid aggregates at differing degrees of maturation. The goal of the present research is to compare the molecular basis of cell damage induced by prefibrillar and fibrillar forms of Aβ 1-40 and Aβ 1-42 aggregates, by checking oxidative stress markers and either apoptotic or necrotic pathway activation in FAD fibroblasts in comparison to healthy cells. This is a new approach to the identification of early modifications in living cells having a genetic drawback in tissues where AD lesions occur. Our results agree with previous evidence from neuronal cells under various experimental conditions. In particular, we found that the cell lines investigated have very different susceptibility to toxic amyloid aggregates, and that the difference in cell viability is related to their ability to: (i) affect the rate of accumulation of amyloid assemblies into the plasma membrane; (ii) prevent oligomeric inclusion; (iii) buffer ROS production.

2. Materials and methods

2.1. Materials

All reagents were of analytical grade or the highest purity available. Unless otherwise stated, chemicals were purchased from Sigma–Aldrich (Milan, Italy). 2′,7′-Dichlorodihydrofluorescein diacetate (CM-H_2, DCFDA) and wheat germ agglutinin-conjugated fluorescein were from Molecular Probes (Eugene, OR). PVDF Immobilio-P Trans-

fer Membrane was obtained from Millipore Corporation (Bedford, MA); Hybond N+ nylon membrane (Amersham, Life Science, England). The rabbit anti caspase-3/CPP32 polyclonal antibody was from Biosource International (Camarillo, CA); secondary antibodies were from Santa Cruz Biotechnology (Santa Cruz, CA). Quantity One program for the image analysis and densitometry was from Biorad (Hercules, CA). Aβ 1-40 and Aβ 1-42 peptides, as trifluoroacetate salts, were purchased from Bachem (Bübendorf, Switzerland). Lyophilized Aβ 1-40 and Aβ 1-42 peptides were stored as powder at −20 °C until reconstitution in phosphate-buffered saline (PBS) without calcium and magnesium, pH 7.2 at a concentration of 230 μM. Reconstituted peptides were stored as aliquots at −20 °C until used. Aβ 1-40 and Aβ 1-42 prefibrillar aggregates were obtained by diluting aliquots of 230 μM stock solutions, thawed at room temperature, in serum free Dulbecco Modified Eagle's Medium (DMEM) and bath sonicated for 5 min to break up any cluster formation before adding to fibroblasts. Otherwise, Aβ 1-40 fibrillar aggregates were prepared by incubating aliquots of 230 μM Aβ 1-40 stock solutions in PBS without calcium and magnesium, pH 7.2 at 37 °C for 48 h, before addition to cultures.

2.2. ThT assay

Aβ 1-40 and Aβ 1-42 peptides were incubated at a concentration of 230 μM in PBS, pH 7.2 at 37 °C. At regular time-intervals 10 μl aliquots of each sample were added to 490 μl of a solution containing 25 μM ThT, 25 mM phosphate buffer, pH 6.0. The steady-state fluorescence values of the resulting samples were measured at 25 °C using a 2 mm × 10 mm path length quartz cuvette and a Perkin-Elmer LS 55 spectrofluorimeter (Wellesley, MA) equipped with a thermostated cell holder attached to a Haake F8 water bath (Karlsruhe, Germany). The excitation and emission wavelengths were 440 and 485 nm, respectively. All measured fluorescence values are given after subtracting the ThT fluorescence intensity measured in the absence of protein and normalized so that the final fluorescence intensity at the endpoint of the kinetic trace was 100%.

2.3. Tapping mode atomic force microscopy (TM-AFM)

20 μl aliquots of Aβ 1-40 and Aβ 1-42 peptides were deposited on freshly cleaved mica substrates and dried under mild vacuum. TM-AFM images were acquired in air using a Dimension 3000 microscope (Digital Instruments, Veeco, Santa Barbara, CA) equipped with a 'G' scanning head (maximum scan size 100 μm) and a Multimode scanning probe microscope equipped with a "E" scanning head (maximum scan size 10 μm). Single beam uncoated silicon cantilevers were used (type OMCL-AC, Olympus, Japan). The drive frequency was around 300 kHz; the scan rate was between 0.3 and 0.8 Hz.

2.4. Cell culture and exposure to Aβ aggregates

In the present study we investigated twelve fibroblast cell lines. Fibroblasts were obtained from four patients belonging to two Italian families bearing the APP Val717Ile mutation (mean ± S.D., age = 55.2 ± 4.5 years) and from four patients belonging to two other Italian families bearing the PS-1 Met146Leu and Leu392Val mutations (mean ± S.D., age = 47.52 ± 9.9 years), respectively. The patient clinical assessment was done according to published guidelines [64] and the AD diagnosis fulfilled the Diagnostic and Statistical Manual of Mental Disorders criteria (DSM-IV) [1]. Four age-matched healthy subjects (mean ± S.D., age = 52.3 ± 8.2 years) were also analyzed. The local ethical committee approved the protocol of the study and written consent was obtained from all subjects or, where appropriate, their caregivers. All control subjects were tested and none of them carried APP or PS-1 mutations. These subjects were also carefully assessed with a rigorous diagnostic evaluation in order to exclude diagnosis of other neurological disorders. Skin biopsies of 3 mm punch were obtained from the volar side of the upper arm of the FAD patients and controls. Two explants were performed from each biopsy and plated in 25-cm^2 flasks. The cells were grown in DMEM, supplemented with 10% foetal bovine serum, and harvested at confluence in T-25 flasks, 7 days after previous subculture. All fibroblast lines were subjected to an equal number of passages (ranging from 10 to 15) and analyzed in three different experiments before confluence. Cultured fibroblasts were exposed to differing concentrations of Aβ 1-40 and Aβ 1-42 prefibrillar aggregates (PF) and of Aβ 1-40 fibrillar aggregates (F), prepared as above described.

2.5. Time-course of Aβ aggregate binding to cell surface membrane

3.5×10^3 $well^{-1}$ healthy and FAD fibroblasts were treated for differing times (0, 10, 20, 30, 60 min) with 1.0 μM Aβ aggregates in a 96-well plate and then washed twice with PBS. The residual aggregate-cell complex was stained with 100 μl of 1.0 μM Congo Red in PBS for 20 min. The Congo Red content was measured photometrically at 490 nm (free Congo Red) and 550 nm (bound Congo Red) with an ELISA plate reader. Under these conditions, the optical density at 550 nm of the Aβ aggregate-Congo Red complex is a measure of the amount of aggregates adsorbed to the cell membrane [22]. Congo Red values are reported as percentage increases *versus* respective untreated fibroblasts (assumed as 100%).

2.6. Internalization of amyloid aggregates

The cells were plated on glass coverslips and incubated with the prefibrillar aggregates of Aβ 1-40 and Aβ 1-42 (PF). Then the cells were counterstained with fluorescein-conjugated wheat germ agglutinin (50 μg/ml) for 15 min to detect plasma membrane profiles and fixed in 2.0%

buffered paraformaldehyde for 10 min at room temperature. Subsequently, permeabilization of plasma membranes was achieved by cell treatment with 3.0% glycerol solution in PBS with a 0.5% bovine serum albumin. In order to verify aggregate internalization, a set of experiments was carried out in the same experimental conditions without glycerol solution in non-permeabilized cells. After washing, the coverslips were incubated with mouse monoclonal anti-Aβ antibodies 6E10 (Signet, DBA, Italy) diluted 1:1000 in PBS with 1% foetal bovine serum for 60 min. The immunoreaction was revealed with Texas Red-conjugated anti-mouse secondary antibodies (Vector Laboratories, DBA, Italy) diluted 1:1000 in PBS with 1% foetal bovine serum for 90 min. Negative controls were obtained by substituting blocking solution for the primary antibody. The fluorescence was analyzed by the confocal Bio-Rad MCR 1024 ES scanning microscope (Hercules, CA) equipped with a krypton/argon laser source (15 mW) for fluorescence measurements using two emission lines at 568 and 488 nm for Texas Red and fluorescein excitation, respectively. Observations were performed using a Nikon Plan Apo 60 × oil immersion objective. A series of optical sections (512 × 512 pixels) 1.0 μm in thickness was taken through the cells at intervals of 0.8 μm. Quantitation of surface bound aggregates and internalized aggregates was achieved by public domain Java image processing program (ImageJ). In particular, fluorescence is expressed as fractional change above the resting baseline, $\Delta F/F$, where F is the average baseline fluorescence before aggregate exposure and ΔF is the fluorescence change over the baseline.

2.7. Measurement of intracellular ROS

Fibroblasts were cultured on glass coverslips and dye loading was achieved by incubating the cells with 5 mM ROS-sensitive fluorescent probe (CM-H_2, DCFDA) for 20 min at 37 °C in the culture medium. DCFH-DA fluorescence into intact cells was detected using a confocal Bio-Rad MCR 1024 ES scanning microscope. A series of optical sections (512 × 512 pixels) was taken through the depth of the cells with a thickness of 1.0 μm at intervals of 0.8 μm. Twenty optical sections for each examined sample were then projected as a single composite image by superimposition.

2.8. Purification of cytosolic fraction

Fibroblasts were washed twice in PBS and harvested in 50 mM Tris–HCl (pH 7.2), containing 0.1 mM phenylmethylsulphonylfluoride (PMSF), 10 μg/ml leupeptine and 10 μg/ml aprotinin prior to storage at −80 °C until use. Rupture of the plasma membrane was achieved by three freeze–thaw cycles followed by centrifugation at 750 × g for 10 min at 4 °C. Cytosolic fractions were used for estimation of total antioxidant capacity (TAC), lipoperoxidation, DNA fragmentation and caspase-3/CPP32. Protein content was measured in cytosolic fractions according to the method of Bradford [5].

2.9. Oxidative markers

Total antioxidant capacity (TAC), accounting for total hydrophilic scavengers, was assayed in cytosolic fractions of cell lysates as reported above by a spectrophotometric method (Total Antioxidant Status, Randox Laboratories LTD., Co. Antrim, UK). Briefly, 2,2′-azino-di-[3-ethylbenzthiazoline sulfonate] (ABTS) was incubated with a peroxidase (metmyoglobin) and H_2O_2 to generate the blue-green radical cation $ABTS^{\bullet+}$ with maximum absorbance at 600 nm. $ABTS^{\bullet+}$ is reduced in the presence of antioxidants proportionally to the concentration of the latter. The results are calibrated using a reference curve based on the soluble antioxidant Trolox (6-hydroxy-2,5,7,8-tetramethylchroman-2-carboxylic acid) as a standard.

To assess the rate of lipid peroxidation, the levels of typical end products of the process: malondialdehyde (MDA) and 4-hydroxyalkenals such as 4-hydroxynonenal (4-HNE) were determined in the cytosolic fraction of cells lysated as specified above. Measurements were made by using a colorimetric method at 586 nm, according to the reaction of the chromogen N-methyl-2-phenylindole, with MDA and 4-HNE in the presence of methanesulfonic acid at 45 °C [24].

2.10. Amyloid cytotoxicity assay

The cytotoxicity of Aβ aggregates was assessed using the 3-(4,5-dimethylthiazol-2-yl)-2,5-diphenyltetrazolium bromide (MTT) assay. Fibroblasts were plated on 96-well plates in 100 μl of fresh medium. Before reaching confluence, the cells were incubated with 100 μl of fresh media without serum in the presence of differing concentrations (0.001, 0.01, 0.1, 1.0, 10 μM) of prefibrillar and fibrillar Aβ 1-40 aggregates or Aβ 1-42 assemblies for 24 h; in time course analysis, cells were exposed to 1 μM amyloid aggregates for 48 and 72 h. The fibroblast culture media were then transferred into a 96-well plates to determine LDH release by using a colorimetric method (Cytotoxicity Detection Kit LDH, Roche Diagnostics) and were immediately replaced with 100 μl of MTT solution in PBS (0.5 mg/ml final concentration). After fibroblast incubation at 37 °C for 4 h, 100 μl of cell lyses buffer (20% SDS, 50% *N*,*N*-dimethylformamide, pH 4.7) was added to each well and the samples were incubated overnight at 37 °C in a humidified incubator. Absorbance values of blue formazan were determined at 590 nm with an automatic plate reader.

2.11. Apoptotic markers

DNA fragmentation, accounting for cell apoptosis, was determined by using an immunometric method (Cell Death

Detection ELISA^{PLUS}, Roche Diagnostics) according to the manufacturer's instructions. DNA fragmentation was expressed as the enrichment of histone-associated oligonucleosomes released to the cytoplasm by measuring the absorption at 405 nm.

Caspase-3 cleavage was measured after 15% SDS-PAGE run of 20 μg proteins. The gels were blotted on PVDF Immobilon-P Transfer Membrane and probed by overnight incubation with rabbit anti caspase-3/CPP32 polyclonal antibodies. This was followed by incubation with the HRP-conjugated secondary antibody and ECL. Band density of the 17 kDa active fragment was measured as densitometric units/μg protein using the image analysis and densitometry program Quantity One.

2.12. Statistical analysis

All data are expressed as mean ± standard deviation (S.D.). Comparison between the different groups were performed by ANOVA followed by Bonferroni *t*-test. A *p*-value less than 0.05 was accepted as statistically significant.

3. Results

3.1. Aβ 1-40 and Aβ 1-42 aggregates

Aβ 1-40 and Aβ 1-42 peptides, as numerous proteins involved in different pathological conditions, convert from their soluble form into highly ordered aggregates referred to as amyloid fibrils [38,61]. These aggregates are typically characterized by a high content of β-structure in which the β-strands are perpendicular to the axis of the fibril and form long β-sheets running along the length of the fibril [23]. The protofibrillar aggregates found in the first stages of the aggregation process bind Thioflavine (ThT), as revealed by an increase in fluorescence intensity following addition of small aliquots of the solution in which they are present.

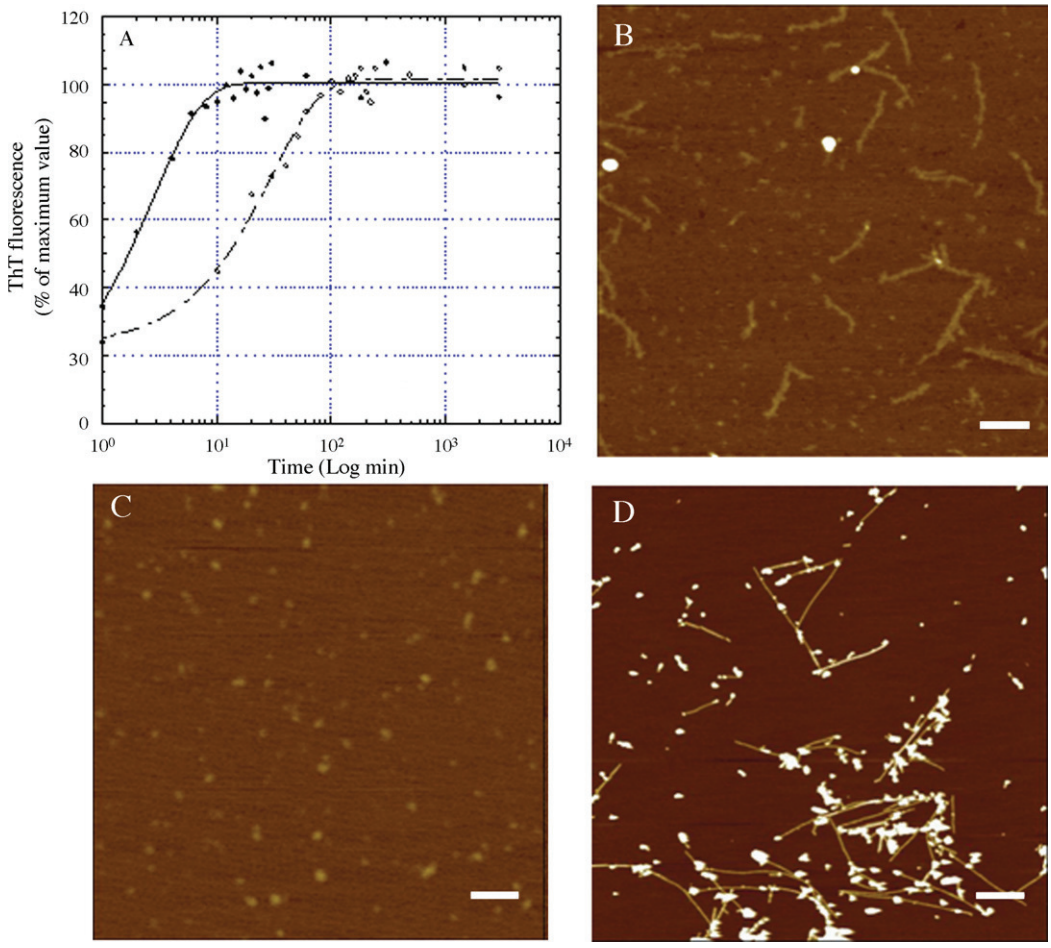

Fig. 1. (A) Time-courses of Aβ 1-40 (empty symbols, dashed line) and Aβ 1-42 (filled symbols, solid line) aggregation measured by ThT fluorescence. The peptides were incubated as described in Section 2. The continuous lines through the data represent the best fits to single exponential function. (B and D) TM-AFM images of prefibrillar and fibrillar structures of Aβ 1-40 taken in air without or with incubation at 37 °C for 48 h, respectively. (C) TM-AFM image of Aβ 1-42 globular aggregates taken in air after Aβ 1-42 dilution. (B) Scan size 1.4 μm, *Z* range 7.8 nm; (C) scan size 672 nm, *Z* range 4.7 nm; (D) scan size 5.0 μm, *Z* range 25 nm. Scale bars represent B, 150 nm; C, 70 nm; D, 500 nm.

Fig. 1A shows the time course of the change of ThT fluorescence as the protein aggregates formed. Whereas the Aβ 1-40 fibrillar aggregates (F) developed after a lag phase, the Aβ 1-42 assemblies reached the maximum ThT fluorescence after few minutes. In addition, aliquots of solutions of Aβ 1-40 and Aβ 1-42 were analyzed using tapping mode atomic force microscopy (TM-AFM) in order to investigate aggregate morphology. As the sample was dried to facilitate its adhesion to the mica substrate, the measured aggregate sizes reported below are reduced with respect to fully hydrated conditions. From previous experiments, the shrinking factor turns out to be 2.0–2.5. In the early stages of the aggregation process, the Aβ 1-40 and Aβ 1-42 aggregates show the morphology typical of protofibrillar structures (PF) (Fig. 1B and C, respectively). Globular structures are observed in both cases: within the experimental error, the globule heights are compatible for Aβ 1-40 and for Aβ 1-42, being 0.5 ± 0.1 and 0.4 ± 0.1 nm, respectively. In our experimental conditions, a small percentage (less than 8%) of the Aβ 1-40 globules displays the tendency to self-assemble into beaded chains composed of several units resembling typical amyloid protofibrils (Fig. 1B). After 48 h of incubation, a significant amount of fibrils (3.1 ± 0.1 nm high) coexisting with globular assemblies, larger (10–15 nm high) than those observed at the early stages of the aggregation, were observed for Aβ 1-40 (Fig. 1D).

3.2. Amyloid aggregates penetrate into fibroblasts

It is widely accepted that cell degeneration in amyloid diseases is mediated by a toxic mechanism involving the interaction of the aggregated species with the plasma membrane of the affected cells [61]. We previously reported a clear increase in membrane lipoperoxidation level in peripheral cells from FAD patients compared to age-matched healthy subjects [15]. Here, we investigate whether the oxidative-damaged membranes of APPV717I fibroblasts enhance the adsorption of the amyloid assemblies on the cellular surfaces. The time-course of aggregate binding to APPV717I and to wild-type cells was performed by exposure for varying lengths of time to 1.0 μM Aβ 1-40 or Aβ 1-42 aggregates; finally the cells were washed with PBS and stained with 1.0 μM Congo Red. It can be seen that, prefibrillar aggregate binding to membranes was considerably earlier and higher in APPV717I than in wild-type fibroblasts (Fig. 2A and C). No significant difference in Congo Red absorbance values between untreated wild-type and APPV717I fibroblasts was observed. The aggregate binding capacity of cells was saturable, reaching its limit in 60 min. An equal cell number from cultures with a comparable division rate from different donors were exposed to the aggregates in order to exclude the influence of these factors on the amount of Aβ bounded to the cell surface. The poor adsorption of Aβ 1-40 mature fibrils to APPV717I fibroblasts was likely due to the presence, in the samples, of minute amounts of residual prefibrillar aggregates, although a specific, yet moderate, fibril binding

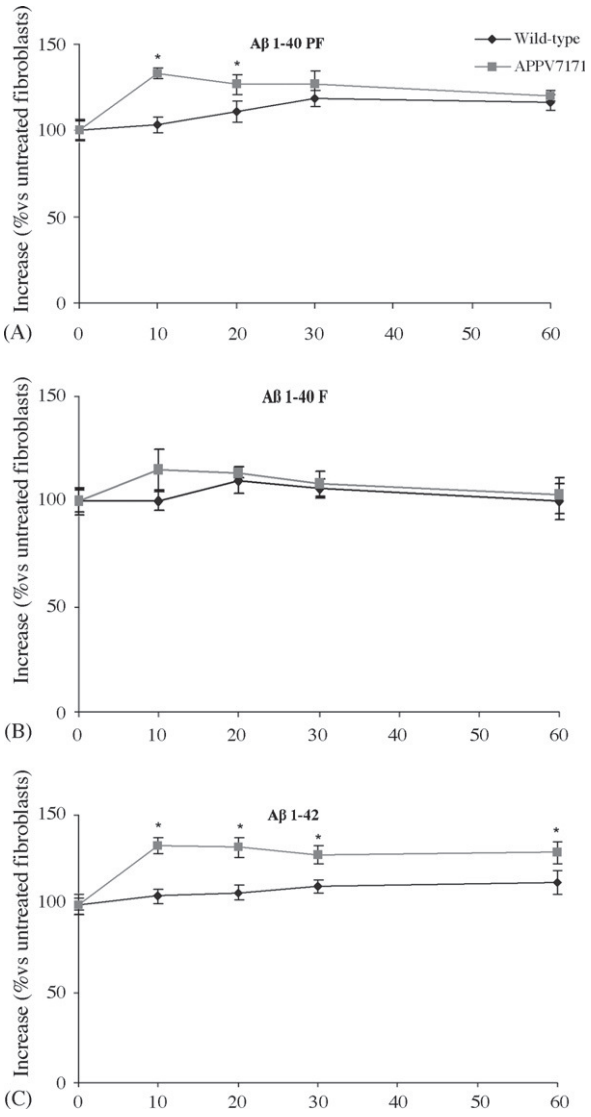

Fig. 2. Time-course of Aβ binding to wild-type and APPV717I fibroblasts. Both cell lines were exposed for 10, 20, 30, 60 min to 1.0 μM Aβ aggregates and then washed twice with PBS. The residual aggregate–cell complex was stained with 1.0 μM Congo Red for 20 min. Under these conditions, Congo Red-staining is a measure of the amount of prefibrillar aggregates adsorbed to cell membrane surface. Wild-type and APPV717I fibroblasts were treated with: (A) Aβ 1-40 PF; (B) Aβ 1-40 F; (C) Aβ 1-42. All values are expressed as means ± S.D. of two independent experiments each carried out in duplicate. No significant difference was observed in the absorbance values measured in untreated fibroblasts (0.049 ± 0.005 in wild-type and 0.047 ± 0.004 in APPV717I). *Significant difference ($p \leq 0.05$) *vs.* wild-type.

cannot be ruled out (Fig. 2B). This evidence is consistent with confocal microscopic analysis at different focal lengths of fibroblasts exposed for 20 and 60 min to the amyloid aggregates. The presence of amyloid aggregates penetrating into the plasma membrane and cytoplasm of fibroblasts was detected by immunofluorescence using monoclonal anti-Aβ antibodies after cell membrane permeabilization with glycerol (Fig. 3A and C). The amyloid oligomers, added to the fibroblast culture medium, accumulate more quickly near the

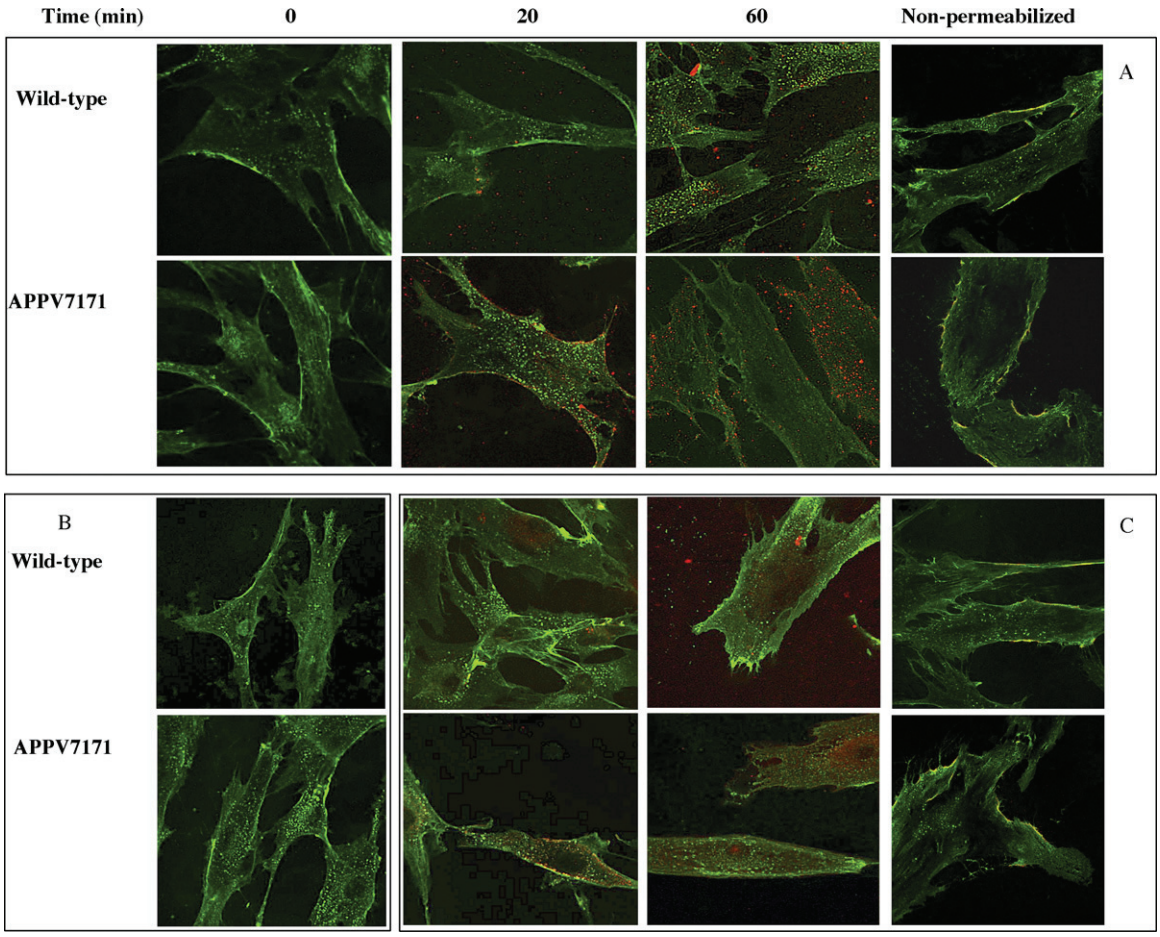

Fig. 3. (A and C) Representative confocal microscopy images showing aggregates in contact with, and penetrating into, the plasma membrane and cytoplasm of fibroblasts after treatment for 0, 20, 60 min with Aβ 1-40 and Aβ 1-42 prefibrillar aggregates, respectively. Counterstaining was performed with fluorescein-conjugated wheat germ agglutinin to detect plasma membrane profile (green). The aggregates were labeled with monoclonal mouse 6E10 anti-Aβ antibodies and Texas Red-conjugated anti-mouse secondary antibodies with or without plasma membrane permeabilization with glycerol as specified under Section 2. Images of a median optical section of 60 min Aβ-treated fibroblasts, non-permeabilized with glycerol, were shown as negative controls of intracellular immunofluorescence signals. (B) Negative control. The cells were incubated with aggregates and then only with secondary antibody without primary antibody.

plasma membrane, and are internalised more rapidly and to a greater extent in APPV717I mutated fibroblasts than in wild-type ones. In contrast, in fibroblasts from healthy subjects just few aggregates following longer time of protein exposure can be observed. Furthermore, Aβ 1-42 assemblies share a more rapid kinetic of interaction with cell surfaces than Aβ 1-40 aggregates in mutated fibroblasts. Images of a median optical section of Aβ-treated fibroblasts, non-permeabilized with glycerol, confirmed that the intracellular immunofluorescence signals, observed in permeabilized cells, are due to internalized aggregates rather than to oligomers bound to cellular surface. Negative controls obtained by incubation of fibroblasts with secondary antibody without primary anti-Aβ antibody verified the specificity of fluorescence signals (Fig. 3B). Cellular confocal analysis of the aggregates directly labeled with Texas Red also confirmed the internalization process into the fibroblasts (data not shown). Quantitation analysis of the amount of aggregates bounded to cell membranes, after 20 min of exposure, and inside the cells, after 60 min of exposure, supported our evidence on the internalization process of Aβ aggregates (Fig. 4). No significant difference in the relative Texas Red fluorescence values between untreated wild-type and APPV717I fibroblasts was observed. To verify internalization data, a Z-series of 0.5 μm optical sections, from the basal to apical surface of APPV717I fibroblasts, was performed by confocal microscopy analysis. As shown in Fig. 5, Aβ 1-42 prefibrillar aggregates were evidently localized within the cells just after 20 min of treatment.

3.3. Oxidative stress

There is strong experimental evidence that oxidative stress is an early biochemical modification in cells facing amyloid aggregates [9,12,54,61]. It is well known that oxidative stress can be caused by increased free radical production and/or weakening of cellular antioxidant defences, which include antioxidant enzymes, lipophilic and hydrophilic scavengers. We have recently found that lymphoblasts and fibroblasts from FAD patients with APPV717I and PS-1 gene mutations had lower basal TAC than healthy controls [15,16]. In the

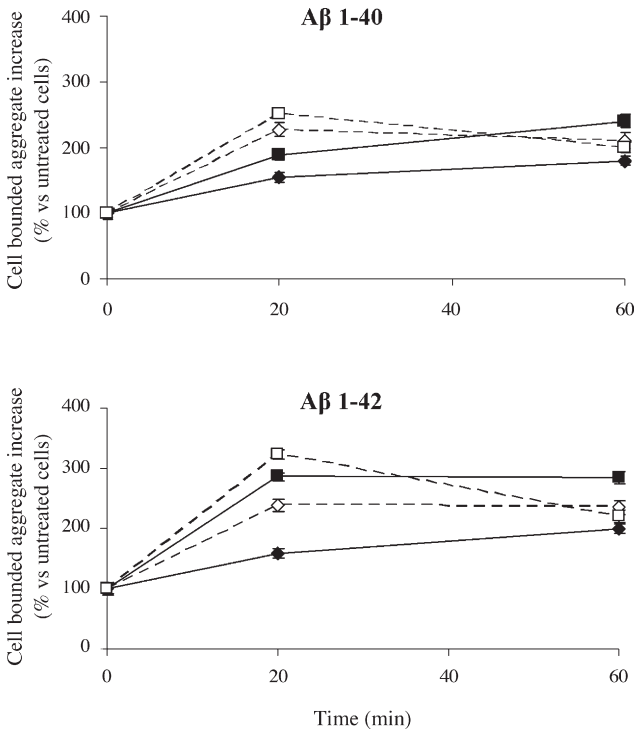

Fig. 4. Time course of the aggregates bounded to surface (empty symbols, dashed line) of wild-type fibroblasts (◊) and APPV717I fibroblasts (□) or aggregate internalization within the cells (filled symbols, solid line). Quantitation analysis of fluorescence signals are expressed as % changes (means ± S.D.) *vs.* respective untreated wild-type (30.2 ± 8.2 fluorescence arbitrary units) and APPV717I (36.3 ± 7.1 fluorescence arbitrary units) fibroblasts (assumed as 100%) of three independent experiments each carried out in duplicate.

present study, we measured the change in non-enzymatic, hydrophilic TAC, relating it to the effect of differing amyloid species. In particular, TAC was affected more by prefibrillar Aβ 1-40 and Aβ 1-42 aggregate treatment in fibroblasts carrying APPV717I mutation than in wild-type cells (Table 1). PS-1 fibroblasts also fell slightly in antioxidant capacity following amyloid aggregate exposure. The reduced ability of APPV717I cells to counteract Aβ aggregate oxidative attack was confirmed by the significant increase in intracellular ROS production in the first 20 min of amyloid aggregate treatment (Fig. 6A–C). Indeed, a time-course confocal analysis of the ROS content showed an earlier and sharper increase in APPV717I fibroblasts than in control cells following either exposure to prefibrillar or fibrillar Aβ 1-40 and Aβ 1-42 aggregates. In particular, ROS increase induced by Aβ 1-40 fibrillar aggregates appears as a result of the internalization of some residual prefibrillar assemblies eventually present in the aggregate solution. A later moderate increase was also clear in control cells after 10 min exposure to Aβ 1-40 prefibrillar structures, and after 20 min exposure to Aβ 1-42 aggregates. ROS accumulation resulted in a clear increase in membrane lipoperoxidation, based on the levels of MDA plus 4-HNE as stable and distinctive final lipoperoxidation products (Table 1). In particular, Aβ 1-42 aggregate exposure induced stronger lipoperoxidation in APPV717I and PS-1 fibroblasts than in wild-type cells.

Table 1
Alterations in antioxidant defences and lipoperoxidation levels induced by amyloid aggregates in APPV717I, PS-1 and wild-type fibroblasts

	TAC	MDA and 4-HNE
Wild-type		
Aβ 1-40 PF	98 ± 14	115 ± 18
Aβ 1-40 F	99 ± 13	106 ± 12
Aβ 1-42	86 ± 16	133 ± 14
APPV717I		
Aβ 1-40 PF	65 ± 12*	144 ± 17*
Aβ 1-40 F	84 ± 11	122 ± 10
Aβ 1-42	48 ± 17*	175 ± 16*
PS-1		
Aβ 1-40 PF	89 ± 10	138 ± 13
Aβ 1-40 F	92 ± 15	114 ± 17
Aβ 1-42	81 ± 11	158 ± 20*

MDA, malondialdehyde; 4-HNE, 4-hydroxy-2-nonenal; TAC, total antioxidant capacity. Values are expressed as pecentage *vs.* untreated fibroblasts. Data are means ± S.D. of three independent experiments, each performed in duplicate.

* $p < 0.05$ with respect to wild-type fibroblasts under the same aggregate treatment.

3.4. Amyloid cytotoxicity

Several recent studies suggest that prefibrillar aggregates arising initially in the path of protein fibrillization are highly cytotoxic, even when they are formed *in vitro* from peptides not associated with protein deposition diseases [7,23,61]. We have previously reported that prefibrillar assemblies of a protein domain, not associated with any disease, are more cytotoxic than mature fibrils to a wide variety of cultured cell lines [14]. In the present study, we first investigated whether the toxicity of prefibrillar Aβ 1-40 aggregates was comparable in fibroblasts carrying APPV717I gene mutation and in age-matched healthy control cells. All cell lines were exposed at 24, 48 and 72 h to 1.0 μM prefibrillar Aβ 1-40 aggregates, and cell viability was then determined by the MTT test. We found that cell viability was lessened in all cells investigated, and that impairment was significantly greater in APPV717I than in control fibroblasts (Fig. 7). In the more susceptible APPV717I fibroblasts, the cytotoxicity depended on the amount of aggregates added for 24 h to the culture media, ranging from 6% at the lowest aggregate concentration (0.001 μM) to 29% at the highest (10 μM) (Fig. 8). In contrast, MTT reduction altered less in APPV717I fibroblasts exposed to 0.001–10 μM mature fibrils. However, the exposure of APPV717I fibroblasts to differing concentrations of Aβ 1-42 aggregates triggered a deeper cytotoxic reaction to Aβ 1-40 prefibrillar and mature fibril Aβ 1-40 assemblies (Fig. 8). Correspondingly, release of cellular LDH into the culture media of both wild-type and APPV717I fibroblasts was greater upon 48 h exposure to 1 μM Aβ 1-42 aggregates than following exposure to prefibrillar and fibrillar Aβ 1-40 species (Fig. 9). In any case, prefibrillar Aβ 1-40 and Aβ

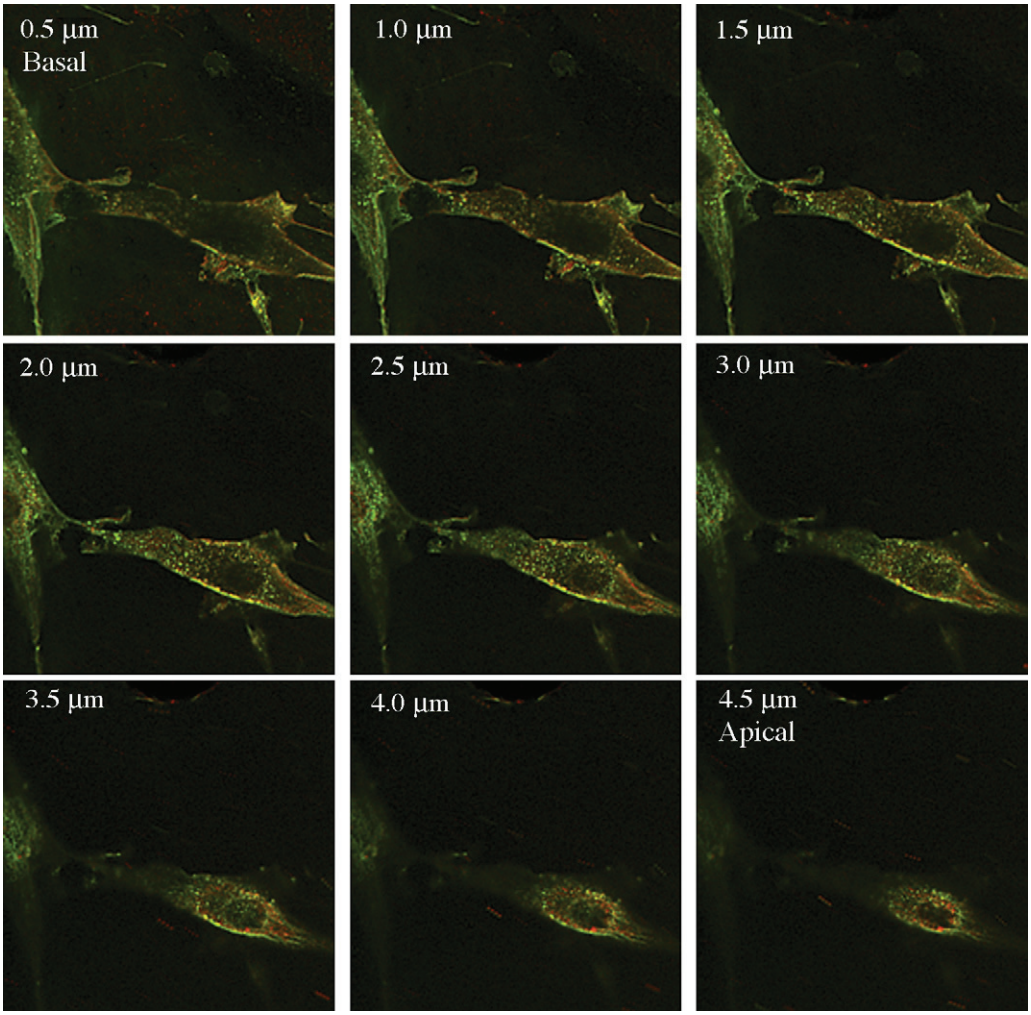

Fig. 5. Aβ 1-42 prefibrillar aggregates are localized within the APPV717I fibroblasts after 20 min treatment. A representative Z-series of 0.5 μm optical sections was taken through cells by confocal microscopy. The aggregates were detected with monoclonal mouse 6E10 anti-Aβ antibodies and Texas Red-conjugated anti-mouse secondary antibodies as specified under Section 2.

1-42 aggregates induced a more significant LDH release in APPV717I fibroblasts than in healthy controls.

3.5. Apoptotic markers

Abundant data indicates that toxicity of amyloid aggregates stems from their ability to interact with cell membranes, triggering apoptotic and/or necrotic cell death [2,3,44,61]. Our previous report found a clear increase in free radical-mediated injury to DNA in FAD fibroblasts relative to healthy controls [15]. In the present study, the observed enrichment of histone-associated oligonucleosomes released to the cytoplasm suggests a greater increase in DNA fragmentation in APPV717I and PS-1 fibroblasts exposed to prefibrillar Aβ 1-42 aggregates than in wild-type cells (Table 2). Involvement of the apoptotic process was confirmed by the increased amount of the caspase-3/CPP32 active fragment (17 kDa) following amyloid exposure. In particular, caspase-3 was raised more in FAD than in wild-type fibroblasts (Table 2).

Table 2
Apoptotic markers in APPV717I, PS-1 and wild-type fibroblasts following amyloid aggregate exposure

	DNA fragmentation	Caspase-3 active fragment
Wild-type		
Aβ 1-40 PF	133 ± 17	119 ± 14
Aβ 1-40 F	111 ± 23	101 ± 13
Aβ 1-42	110 ± 8	111 ± 12
APPV717I		
Aβ 1-40 PF	160 ± 20	232 ± 18*
Aβ 1-40 F	101 ± 13	137 ± 22*
Aβ 1-42	155 ± 15*	182 ± 19*
PS-1		
Aβ 1-40 PF	167 ± 15*	133 ± 13
Aβ 1-40 F	114 ± 10	97 ± 9
Aβ 1-42	134 ± 19*	143 ± 14*

Values are expressed as percentage *vs.* untreated fibroblasts. Data are means ± S.D. of three independent experiments, each performed in duplicate.

* $p < 0.05$ with respect to wild-type fibroblasts under the same aggregate treatment.

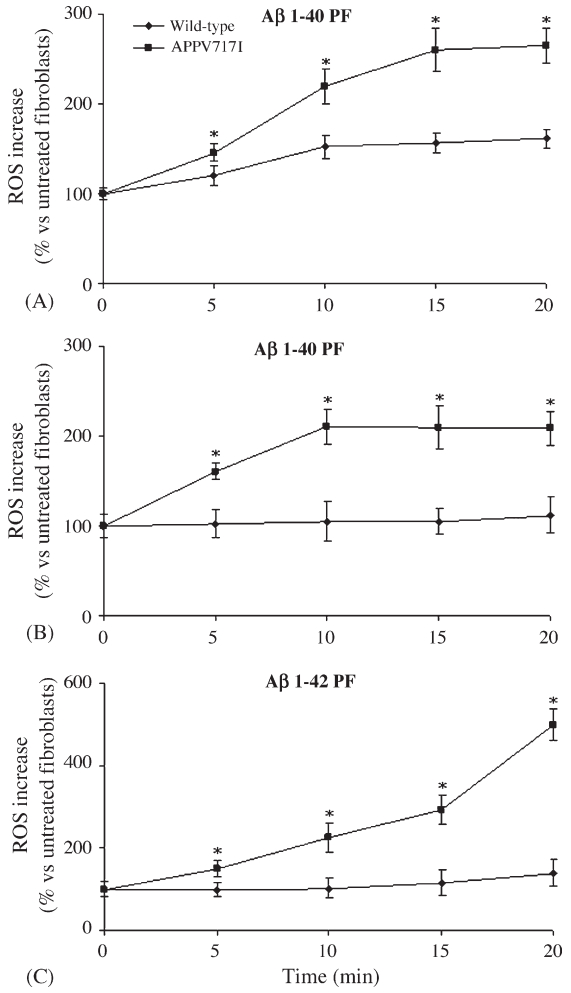

Fig. 6. (A and B) Continuous confocal microscopy analysis of intracellular ROS production in unfixed APP and healthy fibroblasts during the first 20 min treatment with different amyloid aggregates. ROS levels were imaged by confocal microscopy using the fluorescent dye CM-H_2, DCFDA as a probe according to the procedures described under Section 2. Fluorescence signals are expressed as fractional changes above the resting baseline, $\Delta F/F$, where F is the average baseline fluorescence before the application of amyloid aggregates and ΔF represents the fluorescence changes over the baseline. Values are expressed as percentage *vs.* untreated fibroblasts. The values shown are averages ± S.D. of two independent experiments on APPV717I and wild-type fibroblasts from four familial patients and from four healthy subjects, respectively. *Significant difference ($p \leq 0.05$) *vs.* wild-type.

4. Discussion

Several reports provide strong evidence for amyloid lipid peroxidation within the AD brain [10,30,45,48,62,68]. Aβ can fragment and generate free radical peptides which have potent lipoperoxidising effects on the synaptosomal membranes in the neocortex [12,17,32]. However, studies of autopsied brain tissue cannot clarify whether abnormal oxidative processes are inherent properties of AD cells or are secondary to neurodegeneration. Since our previous results showed a marked increase in oxidation levels of lipids and proteins in peripheral cells from some FAD patients [15],

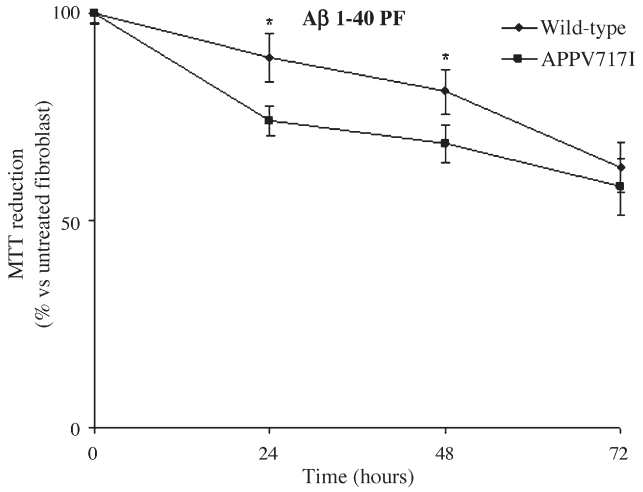

Fig. 7. Cell viability was checked by the MTT test in APPV717I fibroblasts and wild-type fibroblasts exposed to 1.0 μM Aβ 1-40 prefibrillar species *vs.* cells not exposed to the aggregates. Values are expressed as % *vs.* untreated fibroblasts. The reported values (means ± S.D.) are representative of three independent experiments, each performed in duplicate. *Significant difference ($p \leq 0.05$) *vs.* wild-type.

we investigated whether these early modifications could influence the aggregation rate of amyloid assemblies and the translocation process by which the amyloid assemblies appear inside the fibroblasts. Under our experimental conditions, Aβ 1-40 and Aβ 1-42 aggregates are characterized by an extensive β-sheet structure able to bind ThT and are endowed with typical morphological features of prefibrillar and fibrillar aggregates. We demonstrated that amyloid oligomers, that were exogenously added to the fibroblast culture medium, were internalized faster and more completely in APPV717I than in wild-type fibroblasts, although the mechanism of aggregate translocation inside cells needs further investigation. Our results suggest that the amyloid aggregates can readily insert into oxidative-damaged fibroblasts where the membrane integrity is compromised. Accordingly,

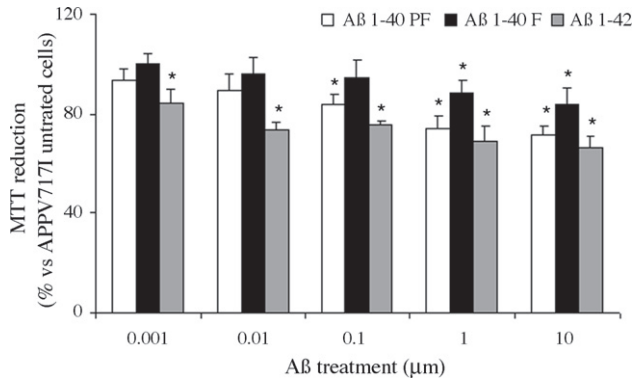

Fig. 8. The figure shows the percentage of viable APPV717I fibroblasts exposed to varying amounts of prefibrillar (PF) or fibrillar (F) Aβ 1-40 and Aβ 1-42 aggregates respect to APPV717I untreated cells. The reported values (means ± S.D.) are expressed as percentage *vs.* untreated fibroblasts and are representative of three independent experiments, each performed in duplicate. *Significant difference ($p \leq 0.05$) *vs.* untreated cells.

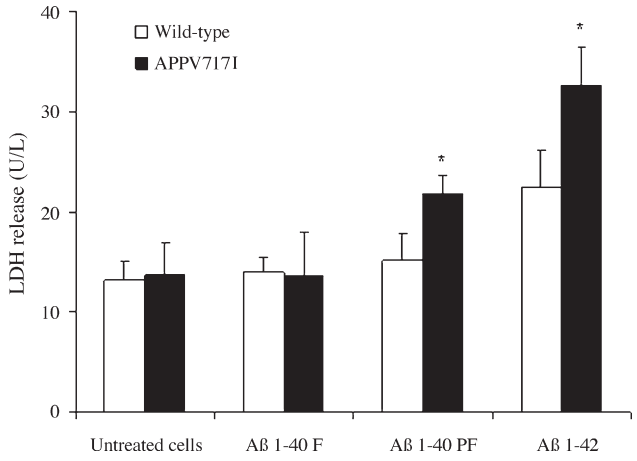

Fig. 9. The release of cellular LDH into the culture media of wild-type and APPV717I fibroblasts without treatment or after 48 h exposure to 1 μM of prefibrillar (PF) or fibrillar (F) Aβ 1-40 and Aβ 1-42 aggregates. The reported values (means ± S.D.) are expressed as percentage *vs.* untreated fibroblasts and are representative of four independent experiments, each performed in duplicate. *Significant difference ($p \leq 0.05$) *vs.* wild-type.

Aβ is reported to accumulate faster in membranes containing oxidatively damaged phospholipids than in membranes containing only unoxidized or saturated phospholipids [39]. Indeed, oxidatively damaged phospholipid membranes promote the transition of Aβ to the β-sheet conformation, which has a strong tendency to form fibrillar aggregates as dense plaques in the brain. It is also possible that APPV717I fibroblasts did not internalize amyloid aggregates unless cellular blebbing was present. Our results, however, are consistent with other previous studies showing intracellular accumulation of Aβ 1-40 and Aβ 1-42 in granular deposits in late endosomes and lysosomes of human fibroblasts, PC12, monocytic and neuroblastoma cell lines [8,37,56,72]. It is increasingly recognized that disruption of the integrity of cell membranes by small prefibrillar assemblies probing into the membrane bilayer is a primary step in the induction of oxidative damage and after cell death [6,23,36,43,57,61]; the early appearance of amyloid aggregates in the cytoplasm of fibroblasts therefore suggests that these species are the main source of oxidative stress for cells. Correspondingly, we found prompt and sharp ROS production in APPV717I fibroblasts exposed to Aβ 1-40 and Aβ 1-42 aggregates. Accordingly, addition of Aβ to PC12 cells induces increased ROS production and apoptosis [12,27,50]. In contrast, treatment of healthy control fibroblasts with small prefibrillar aggregates induced a later and more moderate ROS increase. The significant increase in intracellular ROS production could be induced by a lesser ability of APPV717I cells to counteract Aβ aggregate oxidative attack. Our previous report demonstrated significant impairment in TAC and GSH content in peripheral cells from patients carrying APP or PS-1 mutations, suggesting that a modified redox status is a common feature of cells carrying these genetic lesions [15,16]. In the present study, mutated fibroblasts exhibited larger decreases in TAC following exposure to prefibrillar Aβ 1-40 and Aβ 1-42 aggregates than fibroblasts from healthy subjects. TAC impairment could reflect chronic exposure to an oxidizing environment in mutated fibroblasts with a continuous overproduction of amyloid peptide; it would therefore minimize the protective effect against further oxidative injury following amyloid peptide addition to cellular culture media. The TAC decrease was greater in cells carrying APPV717I than the PS-1 gene mutations. The moderate alteration in TAC in PS-1 mutated fibroblasts strengthens the claim that the changes observed are the direct outcome of the chronic presence of a different grade of cellular oxidizing environment induced by increased Aβ production. Accordingly, we show that addition of Aβ aggregates to the fibroblast culture medium triggers more extensive lipid peroxidation in cells carrying APPV717I or PS-1 gene mutations than in age-matched controls. This effect was stronger in fibroblasts carrying APP rather than PS-1 mutations. Our results therefore suggest that increase in lipid peroxides is likely to result from attack on polyunsaturated fatty acids in cell-membrane phospholipids by free radicals. These findings on peripheral cells are in agreement with several studies that provide evidence for excess lipoperoxidation and protein oxidation associated with Aβ deposits in APP and PS-1 AD brain and mutant mice [9,12,45,51,62]. It has been shown that 4-HNE, generated in response to Aβ-oxidative insults, can directly induce neuronal apoptosis at pathophysiological concentrations [41]. Another study indicates, however, that although free radicals and lipid peroxidation may participate in the neurodegeneration process, the mechanism of Aβ-induced neurotoxicity does not appear to involve ROS [73]. The present observations suggest that prefibrillar Aβ 1-40 aggregates are more toxic than the mature fibrils, and have a dose-dependent effect. Our data are consistent with increasing evidence that small soluble oligomers, compared to mature fibrils, are likely the more toxic species of the peptides [10,11,19,35,38,42,69]. The moderate increase in toxicity with the higher amount of Aβ 1-40 mature fibrils is likely to be the result of minute amounts of residual prefibrillar aggregates in cell media, although a specific toxicity of the fibrils cannot be ruled out. In particular, internalization data of Aβ 1-40 fibrils shown in Fig. 3B, the consequent ROS production reported in Fig. 6B and the cytotoxic effect of Aβ 1-40 fibrils shown in Fig. 8 and Table 2, concurrently suggest that the more structured fibrils maintain some level of direct toxicity. This encourages us to provide for further studies aim to address the potential role of prefibrillar *versus* fibrillar aggregates in mediating these effects. Some authors question the use of the MTT assay as a reporter of Aβ-mediated cytotoxicity [70]. In contrast, according to other researchers, the MTT assay, generally shows a good correlation with other viability tests and *in vivo* results [21]. Therefore, even though inhibition of MTT reduction represents a controversial indicator of Aβ-mediated cell injury, other corroborating evidence was added in this study. Release of cellular LDH into the culture media was specific to the prefibrillar form of Aβ 1-40, because the mature fibrils did not induce toxicity at 48 h after treatment. In any case, prefibrillar Aβ 1-40

and Aβ 1-42 aggregates induced a greater reduction in cell viability and a larger increase in LDH release in APPV717I fibroblasts than in healthy controls. Also, the exposure of APPV717I fibroblasts to differing concentrations of Aβ 1-42 aggregates triggered a deeper cytotoxic reaction respect to prefibrillar Aβ 1-40 aggregates. The earlier accumulation of Aβ1-42 than Aβ1-40 aggregates near the plasma membrane, although similar amount of amyloid assemblies can be internalized at longer time of exposure, can explain the burst in ROS production with a stronger cell viability impairment associated to Aβ1-42 treatment. Anyway, the increasing evidence that Aβ 1-42 is more hydrophobic, more prone to aggregation, and more amyloidogenic than Aβ 1-40 further support the higher cytotoxic effect of Aβ 1-42 peptide. It is well known that the C-terminal hydrophobic tail is likely a crucial feature of Aβ 1-42 cytotoxicity, because of its role in lipid bilayer inclusion [10]. A recent report speculates that both Aβ 1-40 and Aβ 1-42 affect learning but only Aβ 1-42 causes extensive neurodegeneration in Drosophila brain using the GAL4-UAS system [33]. Several studies suggest that amyloid aggregate toxicity can trigger apoptotic and/or necrotic cell death [2,3,16,44,61]. It is generally believed that cell death associated with protein aggregates begins with stimulation of the apoptotic response, although recent data show necrotic rather than apoptotic death in some cases [33,65,67,72]. The biochemistry of cell death following exposure to the toxic amyloid aggregates is still under investigation, but our results support these suggestions. Indeed, despite a marked increase in DNA fragmentation and in the caspase-3 active fragment, necrosis appears to be the later outcome of cell death, at least in APP fibroblasts under Aβ 1-42 aggregate treatment. In addition, there was a greater increase in DNA fragmentation in APP and PS-1 fibroblasts than in wild-type cells following exposure to Aβ 1-42 aggregates. Interestingly, DNA fragmentation was positively correlated with cell impairment or with ROS increase. Since the involvement of caspases has been proposed in amyloid-induced apoptosis in cultured neurons [28,34], we also investigated the activation of caspase-3/CPP32. The amount of caspase-3 active fragment was clearly raised more in FAD than in wild-type fibroblasts. In particular, the effect of prefibrillar Aβ 1-40 and Aβ 1-42 was more powerful than that of fibrillar Aβ 1-40 in both APP and PS-1 cells. The mechanism by which caspase-3 is activated by differing amyloid treatment is yet to be settled. Caspase activation may play a role that is not necessarily related to apoptosis [13,25].

In conclusion, our data demonstrate an early internalization of prefibrillar assemblies and a sharp increase in ROS production induced in APPV717I mutated fibroblasts following exposure to prefibrillar amyloid aggregates. Impairment of antioxidant capacity, lipid peroxidation, mitochondrial dysfunction are all triggered, and apoptotic outcomes such as DNA fragmentation, caspase-3 activation and finally LDH release are induced; the latter is certain following exposure to Aβ 1-42 aggregates. Our results suggest that cells carrying an altered proteolytic APP process, such as APPV717I fibroblasts, have enhanced susceptibility to oxidative stress induced by Aβ exposure, which initially triggers the apoptotic pathway and can ultimately lead to necrosis. This pattern relies on a progressive amplification mechanism of the early reactive free radicals by repeated chain reaction processes in membrane lipids consistent with the age dependence of AD [66]. In contrast, healthy control fibroblasts are more resistant to Aβ-oxidative attack, possibly because of their plasma membrane integrity and powerful antioxidant capacity. This capacity is clearly correlated with the viability of cells, explaining the reduced necrotic outcome in healthy fibroblasts exposed to the aggregates. These findings imply a systemic abnormality in FAD that could be important for the use of peripheral cells in pre-clinical trials of antioxidant drugs. More data on the biochemical modifications of increased susceptibility to amyloid toxicity elicited by mutated cells is needed in order to prevent such outcomes, and to design interventions that aim to restore the resistance of cells affected by aggregates.

Acknowledgements

We thank Dr. Claudio Canale and Dr. Irene Forzoni for technical advice. This study has been supported by grants from the Italian MIUR (project numbers 2002058218_001 and 2005054147_001), from Min.Salute/ISS (no. 4AN/F12) and from the Compagnia di San Paolo, Torino, Italy (ref. no. 2004.0995).

References

[1] American Psychiatric Association. Diagnostic and statistical manual of mental disorders. 4th ed. Washington, DC: American Psychiatric Association; 1994.
[2] Anderson AJ, Pike CJ, Cotman CW. Differential induction of immediate early gene proteins in cultured neurons by β-amyloid (Aβ): association of c-Jun with Aβ-induced apoptosis. J Neurochem 1995;65:1487–98.
[3] Behl C, Davis JB, Klier FG, Schubert D. Amyloid beta peptide induces necrosis rather than apoptosis. Brain Res 1994;645:253–64.
[4] Bokvist M, Lindstrom F, Watts A, Grobner G. Two types of Alzheimer's beta-amyloid (1-40) peptide membrane interactions: aggregation preventing transmembrane anchoring versus accelerated surface fibril formation. J Mol Biol 2004;335:1039–49.
[5] Bradford MM. A rapid and sensitive method for the quantitation of microgram quantities of protein utilizing the principle of protein dye binding. Anal Biochem 1976;72:248–54.
[6] Bucciantini M, Calloni G, Chiti F, Formigli L, Nosi D, Dobson CM, et al. Prefibrillar amyloid protein aggregates share common features of cytotoxicity. J Biol Chem 2004;279:31374–82.
[7] Bucciantini M, Giannoni E, Chiti F, Baroni F, Formigli L, Zurdo J, et al. Inherent toxicity of aggregates implies a common origin for protein misfolding diseases. Nature 2002;416:507–11.
[8] Burdick D, Kosmoski J, Knauer MF, Glabe CG. Preferential adsorption, internalization and resistance to degradation of the major isoform of the Alzheimer's amyloid peptide Aβ 1-42, in differentiated PC12 cells. Brain Res 1997;746:275–84.
[9] Butterfield DA, Drake J, Pocernich C, Castegna A. Evidence of oxidative damage in Alzheimer's disease brain: central role for amyloid beta-peptide. Trends Mol Med 2001;12:7548–54.

[10] Butterfield DA, Bush AI. Alzheimer's amyloid β-peptide (1-42): involvement of methionine residue 35 in the oxidative stress and neurotoxicity properties of this peptide. Neurobiol Aging 2004;25: 563–8.
[11] Butterfield DA. Proteomics: a new approach to investigate oxidative stress in Alzheimer's disease brain. Brain Res 2004;1000:1–7.
[12] Butterifield DA. Amyloid beta-peptide (1-42)-induced oxidative stress and neurotoxicity: implication for neurodegeneration in Alzheimer's disease brain. A review. Free Radic Res 2002;36:1307–13.
[13] Canevari L, Abramov AY, Duchen MR. Toxicity of amyloid beta peptide: tales of calcium, mitochondria, and oxidative stress. Neurochem Res 2004;29:637–50.
[14] Cecchi C, Baglioni S, Fiorillo C, Liguri G, Nosi D, Rigacci S, Bucciantini M, Stefani M. Different cell lines are variously affected by the exposure to prefibrillar amyloid aggregates. J Cell Sci 2005;118:3459–70.
[15] Cecchi C, Fiorillo C, Sorbi S, Latorraca S, Nacmias B, Bagnoli S, et al. Oxidative stress and reduced antioxidant defenses in peripheral cells from familial Alzheimer's patients. Free Radic Biol Med 2002;33:1372–9.
[16] Cecchi C, Latorraca S, Sorbi S, Iantomasi T, Favilli F, Vincenzini MT, et al. Gluthatione level is altered in lymphoblasts from patients with familial Alzheimer's disease. Neurosci Lett 1999;275:152–4.
[17] Christen Y. Oxidative stress and Alzheimer disease. Am J Clin Nutr 2000;71:621S–9S.
[18] Citron M, Westaway D, Xia W, Carlson G, Diehl T, Levesque G, et al. Mutant presenilins of Alzheimer's disease increase production of 42-residue amyloid beta-protein in both transfected cells and transgenic mice. Nat Med 1997;3:67–72.
[19] Cleary JP, Walsh DM, Hofmeister JJ, Shankar GM, Kuskowski MA, Selkoe DJ, et al. Natural oligomers of the amyloid-beta protein specifically disrupt cognitive function. Nat Neurosci 2005;8:79–84.
[20] Cruts M, Van Broeckoven C. Molecular genetics of Alzheimer's disease. Ann Med 1998;30:560–5.
[21] Datki Z, Juhasz A, Galfi M, Soos K, Papp R, Zadori D, et al. Method for measuring neurotoxicity of aggregating polypeptides with the MTT assay on differentiated neuroblastoma cells. Brain Res Bull 2003;62:223–9.
[22] Datki Z, Papp R, Zadori D, Soos K, Fulop L, Juhasz A, et al. In vitro model of neurotoxicity of Abeta 1-42 and neuroprotection by a pentapeptide: irreversible events during the first hour. Neurobiol Dis 2004;17:507–15.
[23] Dobson CM. Protein folding and misfolding. Nature 2003;426: 884–90.
[24] Esterbauer H, Schaur RJ, Zollner H. Chemistry and Biochemistry of 4-hydroxynonenal, malonaldehyde and related aldehydes. Free Radic Biol Med 1991;11:81–128.
[25] Gervais FG, Xu D, Robertson GS, Vaillancourt JP, Zhu Y, Huang J, et al. Involvement of caspases in proteolytic cleavage of Alzheimer's amyloid-beta precursor protein and amyloidogenic A beta peptide formation. Cell 1999;97:395–406.
[26] Green JD, Kreplak L, Goldsbury C, Li Blatter X, Stolz M, Cooper GS, et al. Atomic force microscopy reveals defects within mica supported lipid lilayers induced by the amyloidogenic human amylin peptide. J Mol Biol 2004;342:877–87.
[27] Guo G, Sopher BL, Pham DG, Furukawa K, Robinson N, Martin GM, et al. Alzheimer's presenilin mutation sensitizes neural cells to apoptosis induced by trophic factor withdrawal and amyloid beta-peptide: involvement of calcium and oxyradicals. J Neurosci 1997;17:4212–22.
[28] Harada J, Sugimoto M. Activation of caspase-3 in beta-amyloid-induced apoptosis of cultured rat cortical neurons. Brain Res 1999; 842:311–23.
[29] Hardy J, Selkoe DJ. The amyloid hypothesis of Alzheimer's disease: progress and problems on the road of therapeutics. Science 2002;297:353–6.
[30] Harris ME, Hensley K, Butterfield DA, Leedle RA, Carney JM. Direct evidence of oxidative injury produced by the Alzheimer beta-amyloid peptide (1-40) in cultured hippocampal neurons. Exp Neurol 1995;131:193–202.
[31] Hashimoto M, Rockenstein E, Crews L, Masliah E. Role of protein aggregation in mitochondrial dysfunction and neurodegeneration in Alzheimer's and Parkinson's diseases. Neuromol Med 2003;4: 21–36.
[32] Hensley K, Carney JM, Mattson MP, Aksenova M, Harris M, Wu JF, et al. A model for beta-amyloid aggregation and neurotoxicity based on free radical generation by the peptide: relevance to Alzheimer disease. Proc Natl Acad Sci USA 1994;91:3270–4.
[33] Iijima K, Liu HP, Chiang AS, Hearn SA, Konsolaki M, Zhong Y. Dissecting the pathological effects of human Abeta40 and Abeta42 in Drosophila: a potential model for Alzheimer's disease. Proc Natl Acad Sci USA 2004;101:6623–8.
[34] Jordan J, Galindo MF, Miller RJ. Role of calpain- and interleukin-1 beta converting enzyme-like proteases in the beta-amyloid-induced death of rat hippocampal neurons in culture. J Neurochem 1997;68:1612–21.
[35] Kawahara M, Kuroda Y, Arispes N, Rojas E. Alzheimer's beta-amyloid, human islet amylin and prion protein fragment evoke intracellular free calcium elevations by a common mechanism in a hypothalamic GnRH neuronal cell line. J Biol Chem 2000;275: 14077–83.
[36] Kayed R, Head E, Thompson JL, McIntire TM, Milton SC, Cotman CW, et al. Common structure of soluble amyloid oligomers implies common mechanism of pathogenesis. Science 2003;300: 486–9.
[37] Knauer MF, Soreghan B, Burdick D, Kosmoski J, Glabe CG. Intracellular accumulation and resistance to degradation of the Alzheimer amyloid A4/β protein. Proc Natl Acad Sci USA 1992;89: 7437–41.
[38] Koo EH, Lansbury PT, Kelly LW. Amyloid diseases: abnormal protein aggregation in neurodegeneration. Proc Natl Acad Sci USA 1999;96:9989–90.
[39] Koppaka V, Axelsen PH. Accelerated accumulation of amyloid beta proteins on oxidatively damaged lipid membranes. Biochemistry 2000;39:10011–6.
[40] Kourie JI, Henry CL. Ion channel formation and membrane-linked pathologies of misfolded hydrophobic proteins: the role of dangerous unchaperoned molecules. Clin Exp Pharmacol Physiol 2002;29:741–53.
[41] Kruman I, Bruce-Keller AJ, Bredesen D, Waeg G, Mattson MP. Evidence that 4-hydroxynonenal mediates oxidative stress-induced neuronal apoptosis. J Neurosci 1997;17:5089–100.
[42] Lambert MP, Barlow AK, Chromy BA, Edwards C, Freed R, Liosatos M, et al. Diffusible, nonfibrillar ligands derived from Abeta1-42 are potent central nervous system neurotoxins. Proc Natl Acad Sci USA 1998;95:6448–53.
[43] Lashuel HA, Hartley D, Petre BM, Walz T, Lanbury PT. Neurodegenerative disease: amyloid pores from pathogenic mutations. Nature 2002;418:291.
[44] Loo DT, Copani A, Pike CJ, Whittemore ER, Walencewicz AJ, Cotman CW. Apoptosis is induced by β-amyloid in cultured central nervous system neurons. Proc Natl Acad Sci USA 1993;90: 7951–5.
[45] Lovell MA, Ehmann WD, Butler SM, Markesbery WR. Elevated thiobarbituric acid-reactive substances and antioxidant enzyme activity in the brain in Alzheimer's disease. Neurology 1995;45: 1594–601.
[46] Marcus DL, Thomas C, Rodriguez CL, Simberkoff K, Tsai JS, Strafaci JA, et al. Increased peroxidation and reduced antioxidant enzyme activity in Alzheimer's disease. Exp Neurol 1998;150: 40–4.
[47] Markesbery WR, Carney JM. Oxidative alterations in Alzheimer's disease. Brain Pathol 1999;9:133–46.

[48] Markesbery WR, Lovell MA. 4-Hydroxynonenal, a product of lipid peroxidation, is increased in the brain in Alzheimer's disease. Neurobiol Aging 1998;19:33–6.
[49] Masters CL, Simms G, Weinman NA, Multhaup G, McDonald BL, Beyreuther K. Amyloid plaque core protein in Alzheimer disease and Down syndrome. Proc Natl Acad Sci USA 1985;82:4245–9.
[50] Mattson MP. Oxidative stress, perturbed calcium homeostasis, and immune dysfunction in Alzheimer's disease. J Neurovirol 2002;8:539–50.
[51] Mattson MP. Emerging neuroprotective strategies for Alzheimer's disease: dietary restriction, telomerase activation, and stem cell therapy. Exp Gerontol 2000;35:489–502.
[52] Mattson MP, Guo Q, Furukawa K, Pedersen WA. Presenilins, the endoplasmic reticulum, and neuronal apoptosis in Alzheimer's disease. J Neurochem 1998;70:1–14.
[53] McCormack JG, Halestrap AP, Denton RM. Role of calcium ions in regulation of mammalian intramitochondrial metabolism. Physiol Rev 1990;70:391–425.
[54] Mecocci P, MacGarvey U, Beal MF. Oxidative damage to mitochondrial DNA is increased in Alzheimer's disease. Ann Neurol 1994;36:747–51.
[55] Montine TJ, Neely MD, Quinn JF, Beal MF, Markesbery WR, Roberts LJ, et al. Lipid peroxidation in aging brain and Alzheimer's disease. Free Radic Biol Med 2002;33:620–6.
[56] Morelli L, Prat MI, Castano EM. Differential accumulation of soluble amyloid beta peptides 1-40 and 1-42 in human monocytic and neuroblastoma cell lines. Implications for cerebral amyloidogenesis. Cell Tissue Res 1999;298:225–32.
[57] Orrenius S, Zhovotovsky B, Nicotera P. Regulation of cell death: the calcium-apoptosis link. Nat Rev 2003;4:552–65.
[58] Price DL, Tanzi RE, Borchelt DR, Sisodia SS. Alzheimer's disease: genetic studies and transgenic models. Annu Rev Genet 1998;32:461–93.
[59] Sayre LM, Zelasko DA, Harris PL, Perry G, Salomon RG, Smith MA. 4-Hydroxynonenal-derived advanced lipid peroxidation end products are increased in Alzheimer's disease. J Neurochem 1997;68: 2092–7.
[60] Smith MA, Rudnicka-Nawrot M, Richey PL, Praprotnik D, Mulvihill P, Miller CA, et al. Carbonyl-related post-translational modification of neurofilament protein in the neurofibrillary pathology of Alzheimer's disease. J Neurochem 1995;64:2660–6.
[61] Stefani M, Dobson CM. Protein aggregation and aggregate toxicity: new insights into protein folding, misfolding diseases and biological evolution. J Mol Med 2003;81:678–99.
[62] Subbarao KV, Richardson JS. Autopsy samples of Alzheimer's cortex show increased peroxidation in vitro. J Neurochem 1990;55:342–5.
[63] Takeda K, Araki W, Tabira T. Enhanced generation of intracellular Abeta42 amyloid peptide by mutation of presenilins PS1 and PS2. Eur J Neurosci 2004;19:258–64.
[64] The Dementia Study Group of the Italian Neurological Society Guidelines for the diagnosis of dementia and Alzheimer's disease. Ital J Neurol Sci 2000;21:87–194.
[65] Turmaine M, Raza A, Mahal A, Mangiarini L, Bates GP, Davies SW. Nonapoptotic neurodegeneration in a transgenic mouse model of Huntington's disease. Proc Natl Acad Sci USA 2000;97: 8093–7.
[66] Varadarajan S, Yatin S, Aksenova M, Butterfield DA. Review: Alzheimer's amyloid beta-peptide-associated free radical oxidative stress and neurotoxicity. J Struct Biol 2000;130:184–208.
[67] Velez-Pardo C, Arroyave ST, Lopera F, Castano AD, Jimenez Del Rio MJ. Ultrastructure evidence of necrotic neural cell death in familial Alzheimer's disease brains bearing presenilin-1 E280A mutation. Alzheimer's Dis 2001;3:409–15.
[68] Volicer M. Free radicals in the development of Alzheimer's disease. Neurobiol Aging 1990;11:567–71.
[69] Walsh DM, Klyubin I, Fadeeva JV, Cullen WK, Anwyl R, Wolfe MS, et al. Naturally secreted oligomers of amyloid beta protein potently inhibit hippocampal long-term potentiation in vivo. Nature 2002;416:535–9.
[70] Wogulis M, Wright S, Cunningham D, Chilcote T, Powell K, Rydel RE. Nucleation-dependent polymerization is an essential component of amyloid-mediated neuronal cell death. J Neurosci 2005;25:1071–80.
[71] Xie J, Guo Q. AATF protects neural cells against oxidative damage induced by amyloid β-peptide. Neurobiol Dis 2004;16:150–7.
[72] Yang AJ, Chandswangbhuvana D, Shu T, Henschen A, Glabe CG. Intracellular accumulation of insoluble, newly synthesized Aβ n-42 in amyloid precursor protein-transfected cells that have been treated with Aβ 1-42*. J Biol Chem 1999;274:20650–6.
[73] Yao ZX, Drieu K, Szweda LI, Papadopoulos V. Free radicals and lipid peroxidation do not mediate beta-amyloid-induced neuronal cell death. Brain Res 1999;847:203–10.